

一种实心针静电纺丝装置的场强模拟及优化

刘 健¹, 刘延波^{2,3,4}, BUKHARI Samman hassan², 任 倩², 韦春华³, 蒋秀明¹

(1. 天津工业大学天津市现代机电装备技术重点实验室, 天津 300387;

2. 武汉纺织大学纺织学院, 武汉 430200; 3. 天津工业大学纺织学院, 天津 300387;

4. 天津工业大学先进纺织复合材料教育部重点实验室, 天津 300387)

摘要 提出一种实心针静电纺丝方法, 采用实心针作为静电发射极, 并将其置于由绝缘材料制成的导液棒轴心, 导液棒处于储液盒底部的圆锥沉头通孔内部并可以做升降运动以控制供液量, 需要时还可以起到通流的作用, 有效地解决了多针头静电纺丝堵塞和无针头静电纺丝开放式供液的问题. 利用 COMSOL 有限元分析软件对影响场强大小及分布的各参数进行场强模拟, 研究增大场强并减小边缘效应的改进方法, 并采用研发的不完全齿轮横动机构纺丝头做往复横动进行纺丝实验, 验证了实心针静电纺丝装置有效降低了能耗和边缘效应, 避免了针头堵塞及溶剂挥发问题.

关键词 静电纺丝; 实心针; COMSOL; 电场模拟

中图分类号 O631

文献标志码 A

Electric Field Simulation and Optimization on Solid-core Needles of Electrospinning Device

LIU Jian^{1*}, LIU Yanbo^{2,3,4*}, BUKHARI Samman hassan², REN Qian²,
WEI Chunhua³, JIANG Xiuming¹

(1. Tianjin Key Laboratory of Modern Technology & Equipment, Tianjin Polytechnic University, Tianjin 300387, China;

2. School of Textiles, Wuhan Textile University, Wuhan 430200, China;

3. School of Textiles, Tianjin Polytechnic University, Tianjin 300387, China;

4. Key Laboratory of Advanced Textile Composites, Ministry of Education, Tianjin Polytechnic University, Tianjin 300387, China)

Abstract Electrospinning is a widely used technique for nanofiber preparation at large scale that is mainly divided into two categories, namely, multi-needle and needleless categories. However, both categories have some drawbacks. For example, the capillary channels of the former can easily get jammed, while the solvent in the polymer solution storage box of the latter is liable to volatilize. A new type of solid-core needle electrospinning method was proposed and investigated to overcome the shortcomings of the current electrospinning technology. In this method, the solid-core needles with no capillary channels were used as the emitting electrodes and placed on the axis of the solution guiding rods made of insulating materials. The solution guiding rods were in close connection with the taper holes at the bottom of the solution storage box and could be moved up and down to control the solution flow. Moreover, the reciprocating up-and-down movement of the solution guiding rods can clean up the liquid feeding channels, thereby preventing the solution from coagulating and blocking the channels. Thus, the problems existing in the current electrospinning

收稿日期: 2016-11-29. 网络出版日期: 2017-05-22.

基金项目: 国家自然科学基金(批准号: 51373121)资助.

联系人简介: 刘延波, 女, 博士, 教授, 主要从事超细纤维材料的开发技术研究. E-mail: yanboliu@gmail.com

刘 健, 男, 讲师, 主要从事 CAD/CAM 一体化技术、新型纺织机械设计及理论研究. E-mail: liujian3286@126.com

technologies, such as the needle capillary blockage in the needle electrospinning method and the rapid solvent volatilization in the solution box in the needleless electrospinning method, can be efficiently avoided. Electric field intensity simulations of the newly established electrospinning models were also performed to find the optimum structure parameters by increasing the field intensity and reducing the end effect with the help of the finite element analysis software, COMSOL. Lastly, electrospinning experiments were conducted on the newly invented electrospinning device based on the solid-core needle and non-circular gear traverse mechanism. The results indicate that this new electrospinning method could solve the complications of polymer clogging and solvent volatilization and obtain a uniform electrospinning effect.

Keywords Electrospinning; Solid-core needle; COMSOL; Electric field simulation

Electrospinning is an effective technique to produce nanofiber using an electric field force to stretch the spinning jets from a polymer solution^[1]. Large-scale electrospinning techniques are currently being practiced and categorized as multi-needles (with capillary needles)^[2-4] and needleless electrospinning techniques^[5-19]. However, both categories have some of the following limitations: (1) in multi-needle electrospinning devices, the capillary channels are likely to get jammed; the superposed repulsive forces cause stronger field intensity at the edge needles and comparatively weaker field intensity at the middle needles (*i.e.*, end effect)^[20]; (2) in needleless electrospinning, controlling the size and distribution of fiber diameters is hard, and the solvent easily volatilizes because of the open environment that leads to the change of concentration and affects the spinning quality.

Accordingly, solid-core needles are developed to work as emitting electrodes to overcome the abovementioned problems. These solid-core needles are placed along the axis of the solution guiding rods made up of insulating materials. The solution guiding rods are in close connection with the taper holes at the bottom of the solution storage box and can be moved up and down to control the solution flow. When needed, the movement of the solution guiding rods can poke holes to ultimately and effectively solve the blockage and solvent volatilization problems. In this paper, the geometric parameters of the emitting electrode using solid-core needles were determined to increase the field intensity and reduce the end effect. The end effect was based on the electric field simulation conducted by employing the finite element analysis software, COMSOL. Finally, the electrospinning experiments were performed using the electrospinning device based on the solid-core needle and non-circular gear traverse mechanism^[21]. The results from the electrospinning experiments specify the function, validity, and reliability of the new device. The findings also introduce a new concept of large-scale secure electrospinning at low energy consumption, high efficiency, and stabilization.

1 Preliminary Design of an Electrospinning Emitting Electrode Using Solid-core Needles

An electrospinning emitting electrode using solid-core needles was proposed to solve the clogging problem of the conventional multi-needle technique. This new device was specially designed to protect the polymer solution. The electrospinning emitting electrode using solid-core needles was composed of solid-core needles, metal wire, solution guiding rods, supporting plate, and storage box (Fig.1). The solid-core needles were adjusted to keep the needle eyes at the top to connect the wire. The solution guiding rod was made of an insulating material with a conical bottom, a cylindrical middle section, and a center with a hole. The solid-core needle was in the hole of the solution guiding rod. N holes were placed in a row with equal spaces between the supporting plates (N is a positive integer, and $N \geq 1$). The solution guiding rods were tightly adjusted in the holes. Accordingly, N taper holes were placed in a row with a conical sinking head at the bottom of the storage box. The solution guiding rods were tightly linked with the taper holes at the bottom of the storage box and were driven by the lifting system that can be moved up and down to control the liquid quantity (Fig.2). All the

needles were connected to each other by the metal wire that passed through the needle eyes of all the solid-core needles.

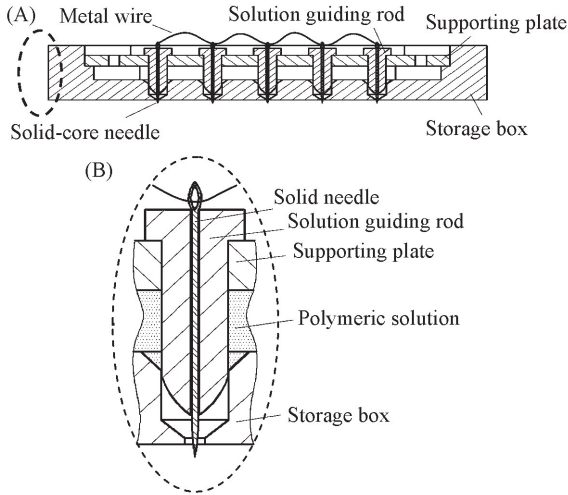


Fig.1 Electrospinning emitting electrode using solid-core needles

(A) Main view; (B) local enlarged view.

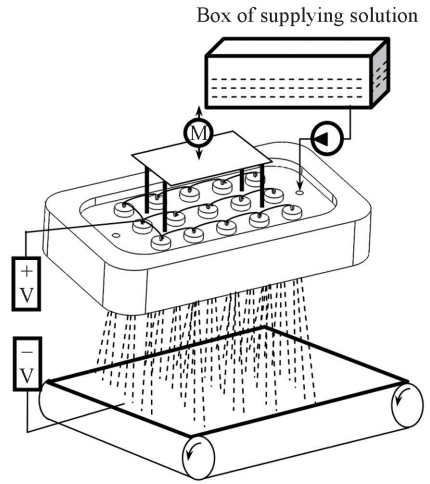


Fig.2 Schematic diagram of the electrospinning device using solid-core needles

Fig.2 shows that the solution guiding rods, which are driven by motor can move up and down when required. This solid-core needle electrospinning device can support mass production by supplying the solution *via* the metering pump.

2 Electric Field Simulation and Determination of Optimum Geometric Parameters

Herein, some measures were taken to understand and tackle the issue of end effect in the conventional multi-needle electrospinning technique. These procedures involved enveloping the solid-core needles in the insulating materials, shortening the length of the solid-core needles, and increasing the diameter of the solution guiding rods, etc. The theoretical simulations of these proposed schemes were performed, and the preliminary structure was optimized.

2.1 Electric Field Simulation

COMSOL multiphysics software was employed to simulate and evaluate the electric field of five needles in a linear array. Table 1 shows the basic parameters of the electrospinning process model. A 30 kV voltage was supplied to the needle of the emitter, and the receiving plate was grounded.

Table 1 Basic model parameters

Voltage/kV	Diameter of needles/mm	Distance between two needles/mm	Receiving distance/mm	Length of needles/mm	Size of receiving plate/mm ³
30	1	28	150	24	150×60×2

Only the result of the emitter was presented to distinctly observe the distribution around the needle tips, considering that the distance between the needle and the receiving plate was large.

2.1.1 Simulation 1: Conventional Five Needles

Fig.3 illustrates the field intensity distribution of five conventional needles. The maximum electric field intensity is 1.97×10^7 V/m, while the focus is on the tips of the needles closer to the receiving plate. Accordingly, the electric field intensity of the needle tip boundary was assessed *via* COMSOL. The average value was calculated and drawn in Fig.4, where the five needles are labeled as 1#, 2#, 3#, 4# and 5#. Fig.4 shows that the electric field intensity at the middle needle is weaker than that at the needles on the edges in the

multi-needle electrospinning technique.

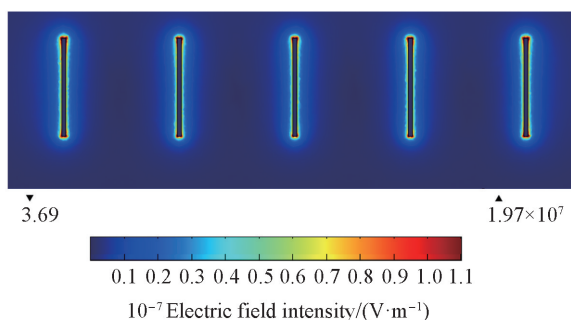


Fig.3 Field intensity map of five conventional needles in a linear array

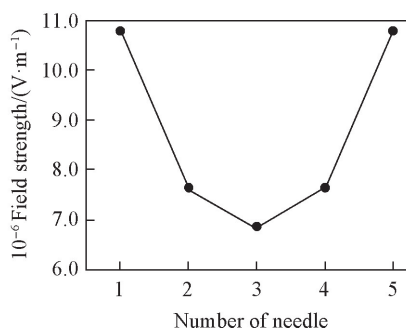


Fig.4 Average electric field intensity of five conventional needles in a linear array

2.1.2 Simulation 2: Five Solid-core Needles in Insulating Materials

The first section depicted that the solid-core needles were inserted into the center holes of the insulating solution guiding rods. In this section, a three-dimensional (3D) model was established and simulated with COMSOL. The solution guiding rods were 24 mm in length and 10 mm in diameter, while the insulating material was made up of polytetrafluoroethylene. Fig.5 shows that the maximum electric field intensity is 2.13×10^7 V/m, which is 8% more than that of the five conventional needles. The average electric field intensity of the needle tips was calculated and drawn in Fig.6.

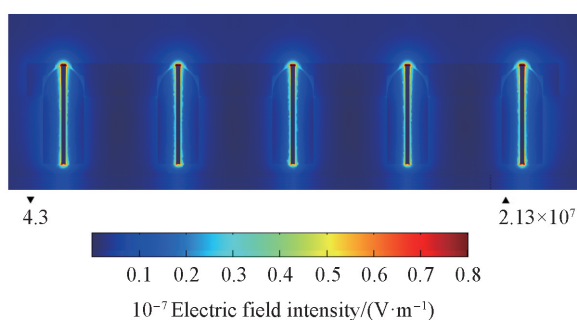


Fig.5 Field intensity map of the solid-core needles wrapped with an insulating material

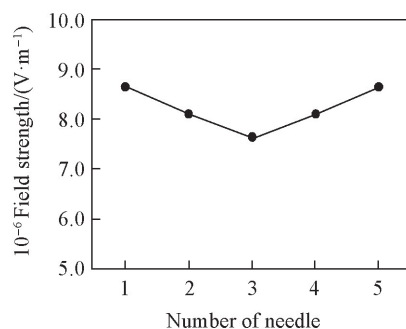


Fig.6 Average electric field intensity of the solid-core needles wrapped with an insulating material

A comparison of Fig.6 and Fig.4 shows that the mutual interference of the electric field among the five needles is reduced, thereby indicating an improved end effect phenomenon^[22].

2.2 Determination of the Optimum Geometric Parameters

Some measures can be taken to further enhance the electric field intensity and reduce the end effect of the solid-core needles. These approaches include shortening the length of solid-core needles, increasing the diameter of the solution guiding rods, and designing the tip of the solid-core needle to a cone shape.

2.2.1 Shortening the Length of the Solid-core Needles

The basic role of the solid-core needle in an electrospinning emitting electrode is to apply voltage to generate an electric field, which can possibly reduce its length. The induced charge concentration is increased, and the electric field intensity is ultimately enhanced, by reducing the length of the solid-core needle. The lengths of the solid-core needles were 24, 12, 6 and 3 mm, respectively. Accordingly, the 3D model and the simulated electric field were established *via* COMSOL. Fig.7 shows the field intensity maps, while Fig.8 illustrates the peak values of the electric field intensity being 2.13×10^7 , 2.57×10^7 , 3.31×10^7 and 3.96×10^7 V/m, respectively.

The average electric field intensity of the five needle tips in the four design lengths were calculated and drawn in Fig.9. Fig.9 shows that the peak value of the electric field intensity increases, and the electric field

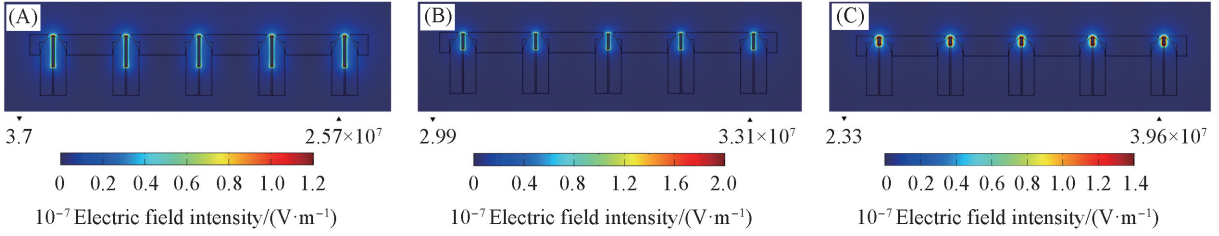


Fig.7 Field intensity maps after changing the length of the solid-core needles
 Length of needles/mm: (A) 12; (B) 6; (C) 3.

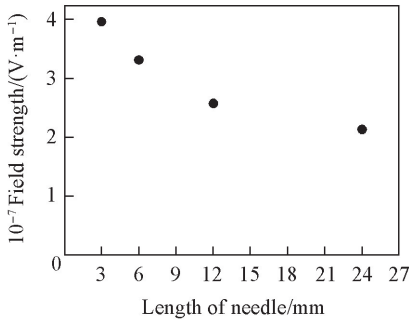


Fig.8 Peak value of the electric field intensity after changing the length of the solid-core needles

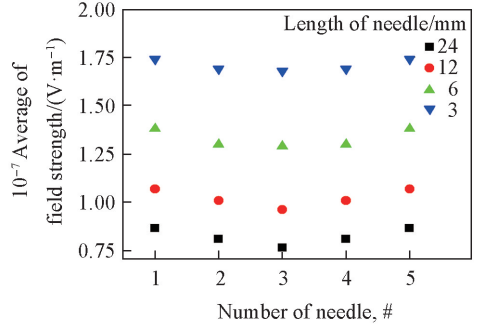


Fig.9 Average electric field intensity after changing the length of the solid-core needles

becomes more uniform, with the reduction of the length of the solid-core needle. However, according to the processing feasibility, a very short solid-core needle is not easy to manufacture. Hence, the 3 mm-long solid-core needle was chosen as the shortest. The maximum electric field intensity is 3.96×10^7 V/m, and it increases by 101% more than the conventional one.

2.2.2 Increasing the Diameter of the Solution Guiding Rods

The diameters of the solution guiding rods were set from 10 mm to 11 and 12 mm. Then, the 3D models were established, and the electric field was simulated with COMSOL. Fig.10 shows the field intensity maps.

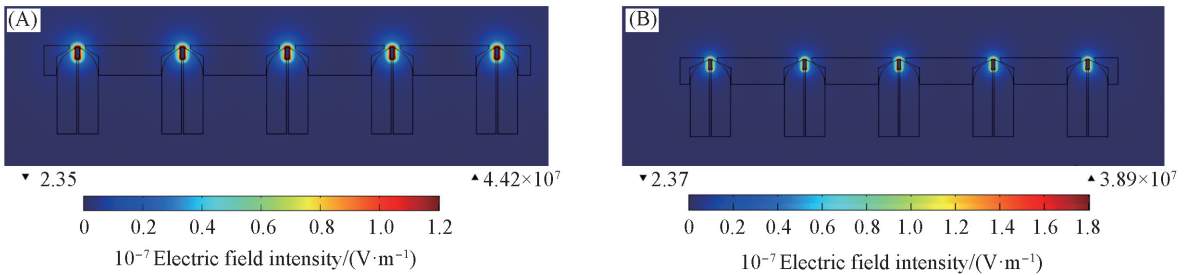


Fig.10 Field intensity maps after increasing the diameter
 Diameter of solution guiding rods/mm: (A) 11; (B) 12.

The peak values of the electric field intensity are 3.96×10^7 , 4.42×10^7 and 3.89×10^7 V/m. Therefore, the optimum diameter of the solution guiding rod is pointed out as 11 mm. The maximum electric field intensity is 4.42×10^7 V/m, 124% more than that for the five conventional needles.

2.2.3 Designing the Tip of the Solid-core Needle to a Cone Shape

Based on the principle of tip discharge under the

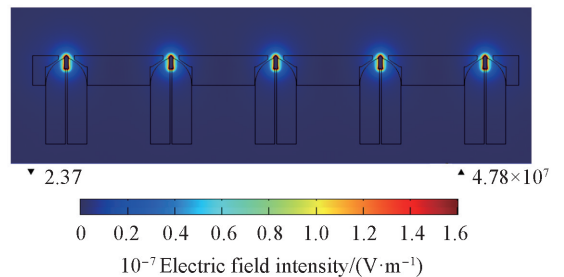


Fig.11 Field intensity map of the solid-core needles with conical tips

same conditions of the conductor's charge and the surrounding environment, the electric field intensity can be enhanced by sharpening the tip of the solid-core needle. Unlike the conventional capillary needle, the tip of the solid-core needle was molded into a cone shape. Subsequently, a 3D model was established, and the electric field was simulated using COMSOL. Fig.11 shows the field intensity map. The peak value of the electric field intensity is 4.78×10^7 V/m, 143% more than that of the five conventional needles.

3 Experimental and Results

3.1 Device

The experiment was performed with an electrospinning device using solid-core needles(Fig.12).

The electrospinning device was self-made and had fifteen solid-core needles. The receiving plate was made of steel with the size of 150 mm×60 mm×2 mm. The type of the DC high-voltage power supply was DW-P/N603(Tianjin Dongwen High Voltage Power Supply, Ltd., China). The power of the metal halide lamp was 70 W and purchased from Xincheng Lighting, Ltd., China. The motor agitator using for preparing polymer solution was DF-101S(Gongyi Yuhua Instrument Co., Ltd., China). The type of the thermostat water bath was HH-4 of the Kexi Instrument, Ltd., China. And the camera which was used to take pictures for spinning process was Sony DSC-TX9.

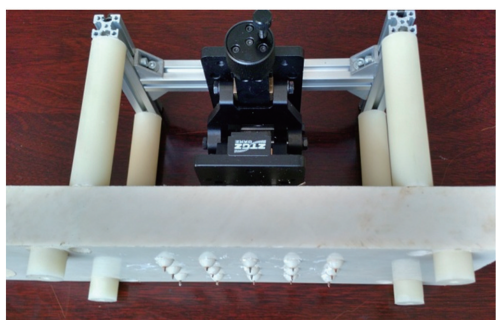


Fig.12 Electrospinning device with solid-core needles

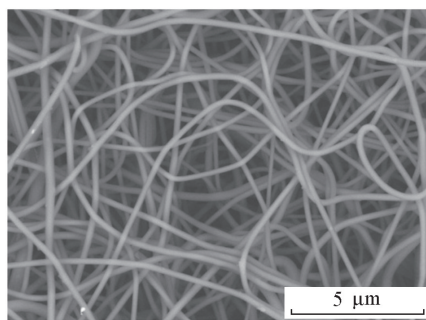


Fig.13 SEM image of nanofibers

3.2 Spinning Solution

Accordingly, a 15% polyvinylidene fluoride(PVDF) solution was prepared. The PVDF was placed in a vacuum drying oven and dried for 12 h at 80 °C. An appropriate amount of PVDF was then weighed and poured into a mixture of solvent dimethylformamide/acetone(volume ratio: 7:3). A magnetic rotor was placed in the solution. Subsequently, the solution was transferred to a thermostatic bath and stirred at 50 °C until the solution was clear and transparent.

3.3 Parameters

A DC power of 20 kV was supplied by the positive voltage to the solid-core needles, while a negative voltage of 5 kV was applied to the receiving electrode. The receiving distance was 150 mm. The feeding rate of each needle was approximately 10 mL/h, and the spinning time was 15 min.

3.4 Results

The nanofiber film of PVDF with an average diameter of 115 nm and a CV value of 12% was obtained *via* the electrospinning experiment. Fig.13 shows its scanning electron microscopy(SEM) image.

4 Conclusions

Compared to the conventional capillary multi-needle device, the designed electrospinning device with solid-core needles has the following advantages. The shorter length and the conical tip of the solid-core needles increased the charging density and produced the enhanced electric field, thereby resulting in the less energy wastage. The solid-core needles were wrapped with insulating solution guiding rods that reduced the

electrostatic repulsion among the needles. A uniform electric field intensity was also achieved. The solution guiding rods were in close connection with the taper holes at the bottom of the liquid storage box and can be moved up and down to control the liquid supply. The movement of the solution guiding rods can poke holes when needed, thereby effectively solving the clogging and volatilization problems.

This paper is supported by the National Natural Science Foundation of China(No.51373121).

References

- [1] Huang X. P., *Experimental Study on Mass-spun Nanofibers Through Tip-less Electrospinnig*, Xiamen University, Xiamen, **2008**
- [2] Tomaszewski W., Szadkowski M., *Fibres. Text. East. Eur.*, **2005**, 13(4), 22—26
- [3] Theron S. A., Yarin A. L., Zussman E., Kröll E., *Polymer*, **2005**, 46(9), 2889—2899
- [4] Varesano A., Carletto R. A., Mazzuchetti G., *J. Mater. Process Tech.*, **2009**, 209(11), 5178—5185
- [5] Wang F. L., Shao Z. S., *China Textile Leader*, **2014**, 1, 64—67
- [6] Xie G., Song Q. S., Deng D. P., Liu Y., *Eng. Plast. Appl.*, **2014**, 6(42), 117—122
- [7] Niu H. T., Wang X., Lin T., *Intech.*, **2011**, 11, 17—36
- [8] Jirsak O., Sanetrik F., Lukas D., Kotek V., Martinova L., *A Method of Nanofibres Production from a Polymer Solution Using Electrostatic Spinning and a Device for Carrying out the Method*, EP 1673493B1, 2009-08-07
- [9] Huang X. P., Wu D. Z., Zhu Y. Y., Sun D., *IEEE-NANO*, **2007**, 45(9), 823—826
- [10] Niu H. T., Lin T., Wang X. G., *J. Appl. Polym. Sci.*, **2009**, 114(6), 3524—3530
- [11] Wang X., Wang X. G., Lin T., *J. Mater. Res.*, **2012**, 27(23), 3013—3019
- [12] Wang X., Niu H. T., Wang X. G., Lin T., *J. Nanomater.*, **2012**, 785920(10), 1875—1890
- [13] Wang X., Niu H. T., Lin T., Wang X. G., *Polym. Eng. Sci.*, **2009**, 49(8), 1582—1586
- [14] Lu B., Wang Y., Liu Y., Duan H., Zhou J., *Small*, **2010**, 6(15), 1612—1616
- [15] Thoppey N. M., Bochinski J. R., Clarke L. I., Gorga R. E., *Polymer*, **2010**, 51(21), 4928—4936
- [16] Thoppey N. M., Gorga R. E., Bochinski J. R., Clarke L. I., *Macromolecules*, **2012**, 45(16), 6527—6537
- [17] Jiang G., Zhang S., Qin X., *Mater. Lett.*, **2013**, 106, 56—58
- [18] Yarin A. L., Zussman E., *Polymer*, **2004**, 45(9), 2977—2980
- [19] He J. H., Liu Y., Xu L., Yu J. Y., Sun G., *Chaos. Soliton Fract.*, **2008**, 37(3), 643—651
- [20] Rulison A. J., Flagan R. C., *Rev. Sci. Instrum.*, **1993**, 64(3), 683—686
- [21] Liu J., Liu Y. B., Jiang X. M., Ma Y., Song X. L., *Text. Res. J.*, **2015**, 36(7), 116—120
- [22] Guo L. L., Liu Y. B., Zhang Z. R., Ma Y., *TJPU J.*, **2012**, 31(2), 23—26

(Ed.: Y, Z, A)